Archive of Applied Mechanics 74 (2005) 526–535 © Springer-Verlag 2005
DOI 10.1007/s00419-004-0369-y

The behavior of a crack in functionally graded piezoelectric/piezomagnetic materials under anti-plane shear loading

Z.-G. Zhou, L.-Z. Wu, B. Wang

Summary In this paper, the behavior of a crack in functionally graded piezoelectric/piezomagnetic materials subjected to an anti-plane shear loading is investigated. To make the analysis tractable, it is assumed that the material properties vary exponentially with the coordinate parallel to the crack. By using a Fourier transform, the problem can be solved with the help of a pair of dual integral equations in which the unknown variable is the jump of the displacements across the crack surfaces. These equations are solved using the Schmidt method. The relations among the electric displacement, the magnetic flux and the stress field near the crack tips are obtained. Numerical examples are provided to show the effect of the functionally graded parameter on the stress intensity factors of the crack.

Keywords Functionally graded piezoelectric/piezomagnetic materials, Schmidt method, Dual integral equations, Crack

1 Introduction

Composite material consisting of a piezoelectric phase and a piezomagnetic phase has drawn significant interest in recent years due to the rapid development in adaptive material systems. It shows a remarkably large magnetoelectric coefficient, the coupling coefficient between the static electric and magnetic fields, which does not exist in either constituent. In some cases, the coupling effect in piezoelectric/piezomagnetic materials can even be a hundred times larger than that in single-phase magnetoelectric materials. Consequently, they are extensively used as electric packaging, sensors and actuators, e.g., magnetic field probes, acoustic/ultrasonic devices, hydrophones and transducers responsible for electro-magneto-mechanical energy conversion [1]. When subjected to mechanical, magnetic and electrical loads in service, these magneto-electro-elastic materials can fail prematurely due to some defects, e.g. cracks, holes, etc., arising during their manufacturing processes. Therefore, it is of great importance to study the magneto-electro-elastic interaction and fracture behaviors of magneto-electro-elastic composites [2, 3]. The development of piezoelectric/piezomagnetic composites has its roots in the early work of van Suchtelen [4] who proposed that the combination of piezoelectric/piezomagnetic phases may exhibit a new material property – the magnetoelectric coupling effect. Since then, few researchers have studied the magnetoelectric coupling effect in composites, and most published research results were obtained in recent years [1–3, 5, 10]. On the other hand, the development of functionally graded materials has demonstrated that they have the potential to reduce the stress concentration and increase fracture toughness. Consequently, the concept of functionally graded materials can be extended to the

Received 4 August 2004; accepted for publication 18 November 2004

Z.-G. Zhou (✉), L.-Z. Wu, B. Wang
P.O. Box 1247, Center for Composite Materials,
Harbin Institute of Technology, Harbin 150001, P.R. China,
e-mail: zhouzhg@hit.edu.cn

The authors are grateful for financial support from the Natural Science Foundation of Hei Long Jiang Province (A0301), the National Natural Science Foundation of China (50232030, 10172030), the Natural Science Foundation with Excellent Young Investigators of Hei Long Jiang Province(JC04-08) and the National Science Foundation with Excellent Young Investigators (10325208).

piezoelectric/piezomagnetic materials to improve the reliability of piezoelectric/piezomagnetic materials and structures. Some applications of functionally graded piezoelectric materials have been made [11, 12]. Recently, the fracture problems of functionally graded piezoelectric materials have been considered [13–17]. However, relatively few works on the crack problem in functionally graded piezoelectric/piezomagnetic materials have been carried out. To our knowledge, the electro-elastic behavior of functionally graded piezoelectric/piezomagnetic materials with a crack subjected to an anti-plane shear loading has not been studied by using the Schmidt method [18–20]. Thus, the present work is an attempt to fill this requirement. Here, we just attempt to give a theoretical solution for this problem.

In this paper, we attempt to extend the concept of functionally graded materials to piezoelectric/piezomagnetic materials. The magneto-electro-elastic behavior of a crack in functionally graded piezoelectric/piezomagnetic materials subjected to an anti-plane shear stress loading is investigated using the Schmidt method [18–20]. The Fourier transform is applied and a mixed boundary-value problem is reduced to a pair of dual integral equations. To solve the dual integral equations, the jump of the displacements across the crack surfaces is expanded in a series of Jacobi polynomials. This process is quite different from that adopted in previous works [1–6, 8–17]. Numerical solutions are obtained for the stress intensity factors for permeable crack surface conditions.

2
Formulation of the problem

It is assumed that there is a crack of length $2l$ in functionally graded piezoelectric/piezomagnetic material planes, as shown in Fig. 1. The functionally graded piezoelectric/piezomagnetic materials' boundary-value problem for anti-plane shear is considerably simplified if we consider only the out-of-plane displacement, the in-plane electric fields and the in-plane magnetic fields. As discussed in [21], since no opening displacement exists for the present anti-plane problem, the crack surfaces can be assumed to be in perfect contact. Accordingly, the electric potential, the magnetic potential, the normal electric displacement and the magnetic flux are assumed to be continuous across the crack surfaces. So, the boundary conditions of the present problem are (in this paper, we just consider the perturbation fields):

$$\begin{cases} \tau_{yz}^{(1)}(x,0^+) = \tau_{yz}^{(2)}(x,0^-) = -\tau_0(x), & |x| \le l \\ w^{(1)}(x,0^+) = w^{(2)}(x,0^-), & |x| > l \end{cases} \tag{1}$$

$$\begin{cases} \tau_{yz}^{(1)}(x,0^+) = \tau_{yz}^{(2)}(x,0^-) \\ \phi^{(1)}(x,0^+) = \phi^{(2)}(x,0^-), \quad D_y^{(1)}(x,0^+) = D_y^{(2)}(x,0^-)\ , \quad |x| \le \infty \\ \psi^{(1)}(x,0^+) = \psi^{(2)}(x,0^-), \quad B_y^{(1)}(x,0^+) = B_y^{(2)}(x,0^-) \end{cases} \tag{2}$$

$$w^{(1)}(x,y) = w^{(2)}(x,y) = 0 \quad \text{for } (x^2+y^2)^{1/2} \to \infty \tag{3}$$

where $\tau_{zk}^{(i)}$, $D_k^{(i)}$ and $B_k^{(i)}$ $(k = x, y, i = 1, 2)$ are the anti-plane shear stress, in-plane electric displacement and in-plane magnetic flux, respectively. $w^{(i)}$, $\phi^{(i)}$ and $\psi^{(i)}$ are the mechanical displacement, the electric potential and the magnetic potential, respectively. In this paper, $\tau_0(x)$ is the anti-plane shear loading. Also, note that all quantities with superscript $i (i = 1, 2)$ refer to the upper half plane 1 and the lower half plane 2, as shown in Fig. 1

Crack problems in nonhomogeneous piezoelectric/piezomagnetic materials do not appear to be analytically tractable for arbitrary variations of material properties. Usually, one tries to generate the forms of nonhomogeneities for which the problem becomes tractable. Similar to the treatment of the crack problem for isotropic nonhomogeneous materials in [22–24], we assume that the material properties are described by

$$c_{44} = c_{440}\mathrm{e}^{\beta x}, \quad e_{15} = e_{150}\mathrm{e}^{\beta x}, \quad \varepsilon_{11} = \varepsilon_{110}\mathrm{e}^{\beta x}, \quad q_{15} = q_{150}\mathrm{e}^{\beta x}, \quad d_{11} = d_{110}\mathrm{e}^{\beta x}, \quad \mu_{11} = \mu_{110}\mathrm{e}^{\beta x} \tag{4}$$

where c_{440} is the shear modulus, e_{150} is the piezoelectric coefficient, ε_{110} is the dielectric parameter, q_{150} is the piezomagnetic coefficient, d_{110} is the electromagnetic coefficient, μ_{110} is the magnetic permeability and β is the functionally graded parameter.

It is assumed that the magneto-electro-elastic material is transversely isotropic. So, the constitutive equations for the mode-III crack in the magneto-electro-elastic material can be

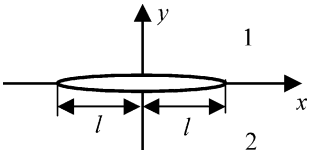

Fig. 1. A crack in functionally graded piezoelectric/piezomagnetic material

expressed as

$$\tau_{zk}^{(i)} = c_{44} w_k^{(i)} + e_{15} \phi_k^{(i)} + q_{15} \psi_k^{(i)}, \quad (k = x, y, \quad i = 1, 2) \tag{5}$$

$$D_k^{(i)} = e_{15} w_k^{(i)} - \varepsilon_{11} \phi_k^{(i)} - d_{11} \psi_k^{(i)}, \quad (k = x, y, \quad i = 1, 2) \tag{6}$$

$$B_k^{(i)} = q_{15} w_k^{(i)} - d_{11} \phi_k^{(i)} - \mu_{11} \psi_k^{(i)}, \quad (k = x, y, \quad i = 1, 2) \tag{7}$$

The anti-plane governing equations are

$$c_{440} \left(\nabla^2 w^{(i)} + \beta \frac{\partial w^{(i)}}{\partial x} \right) + e_{150} \left(\nabla^2 \phi^{(i)} + \beta \frac{\partial \phi^{(i)}}{\partial x} \right) + e_{150} \left(\nabla^2 \psi^{(i)} + \beta \frac{\partial \psi^{(i)}}{\partial x} \right) = 0 \tag{8}$$

$$e_{150} \left(\nabla^2 w^{(i)} + \beta \frac{\partial w^{(i)}}{\partial x} \right) - \varepsilon_{110} \left(\nabla^2 \phi^{(i)} + \beta \frac{\partial \phi^{(i)}}{\partial x} \right) - d_{110} \left(\nabla^2 \psi^{(i)} + \beta \frac{\partial \psi^{(i)}}{\partial x} \right) = 0 \tag{9}$$

$$q_{150} \left(\nabla^2 w^{(i)} + \beta \frac{\partial w^{(i)}}{\partial x} \right) - d_{110} \left(\nabla^2 \phi^{(i)} + \beta \frac{\partial \phi^{(i)}}{\partial x} \right) - \mu_{110} \left(\nabla^2 \psi^{(i)} + \beta \frac{\partial \psi^{(i)}}{\partial x} \right) = 0 \tag{10}$$

where $\nabla^2 = \partial^2/\partial x^2 + \partial^2/\partial y^2$ is the two-dimensional Laplace operator.

3 Solutions

The system of the governing equations above is solved using the Fourier integral transform. The general expressions for the displacement components, the electric potential and the magnetic potential can be written as follows:

$$\begin{cases} w^{(1)}(x, y) = \frac{1}{2\pi} \int_{-\infty}^{\infty} A_1(s) \mathrm{e}^{-\gamma y} \mathrm{e}^{-isx} \mathrm{d}s \\ \phi^{(1)}(x, y) = a_0 w^{(1)}(x, y) + \frac{1}{2\pi} \int_{-\infty}^{\infty} B_1(s) \mathrm{e}^{-\gamma y} \mathrm{e}^{-isx} \mathrm{d}s, \quad (y \geq 0) \\ \psi^{(1)}(x, y) = a_1 w^{(1)}(x, y) + \frac{1}{2\pi} \int_{-\infty}^{\infty} C_1(s) \mathrm{e}^{-\gamma y} \mathrm{e}^{-isx} \mathrm{d}s \end{cases} \tag{11}$$

$$\begin{cases} w^{(2)}(x, y) = \frac{1}{2\pi} \int_{-\infty}^{\infty} A_2(s) \mathrm{e}^{\gamma y} \mathrm{e}^{-isx} \mathrm{d}s \\ \phi^{(2)}(x, y) = a_0 w^{(2)}(x, y) + \frac{1}{2\pi} \int_{-\infty}^{\infty} B_2(s) \mathrm{e}^{\gamma y} \mathrm{e}^{-isx} \mathrm{d}s, \quad (y \leq 0) \\ \psi^{(2)}(x, y) = a_1 w^{(2)}(x, y) + \frac{1}{2\pi} \int_{-\infty}^{\infty} C_2(s) \mathrm{e}^{\gamma y} \mathrm{e}^{-isx} \mathrm{d}s \end{cases} \tag{12}$$

where $A_1(s), B_1(s), C_1(s), A_2(s), B_2(s)$ and $C_2(s)$ are unknown functions, $\gamma = \sqrt{s^2 + is\beta}$, (Re $\lambda \geq 0$), $a_0 = (\mu_{11} e_{15} - d_{11} q_{15})/(\varepsilon_{11} \mu_{11} - d_{11}^2)$, $a_1 = (q_{15} \varepsilon_{11} - d_{11} e_{15})/(\varepsilon_{11} \mu_{11} - d_{11}^2)$.

So from Eqs. (5)–(7), we have

$$\tau_{yz}^{(1)}(x, y) = -\frac{\mathrm{e}^{\beta x}}{2\pi} \int_{-\infty}^{\infty} \gamma [(c_{440} + a_0 e_{150} + a_1 q_{150}) A_1(s) + e_{150} B_1(s) + q_{150} C_1(s)] \mathrm{e}^{-\gamma y} \mathrm{e}^{-isx} \mathrm{d}s \tag{13}$$

$$D_y^{(1)}(x, y) = \frac{\mathrm{e}^{\beta x}}{2\pi} \int_{-\infty}^{\infty} \gamma [\varepsilon_{110} B_1(s) + d_{110} C_1(s)] \mathrm{e}^{-\gamma y} \mathrm{e}^{-isx} \mathrm{d}s \tag{14}$$

$$B_y^{(1)}(x, y) = \frac{\mathrm{e}^{\beta x}}{2\pi} \int_{-\infty}^{\infty} \gamma [d_{110} B_1(s) + \mu_{110} C_1(s)] \mathrm{e}^{-\gamma y} \mathrm{e}^{-isx} \mathrm{d}s \tag{15}$$

$$\tau_{yz}^{(2)}(x,y)=\frac{e^{\beta x}}{2\pi}\int_{-\infty}^{\infty}\gamma[(c_{440}+a_0e_{150}+a_1q_{150})A_2(s)+e_{150}B_2(s)+q_{150}C_2(s)]e^{\gamma y}e^{-isx}ds \tag{16}$$

$$D_y^{(2)}(x,y)=-\frac{e^{\beta x}}{2\pi}\int_{-\infty}^{\infty}\gamma[\varepsilon_{110}B_2(s)+d_{110}C_2(s)]e^{\gamma y}e^{-isx}ds \tag{17}$$

$$B_y^{(2)}(x,y)=-\frac{e^{\beta x}}{2\pi}\int_{-\infty}^{\infty}\gamma[d_{110}B_2(s)+\mu_{110}C_2(s)]e^{\gamma y}e^{-isx}ds \tag{18}$$

To solve the problem, the jump of the displacements across the crack surfaces is defined as follows:

$$f(x)=w^{(1)}(x,0^+)-w^{(2)}(x,0^-) \tag{19}$$

Substituting Eqs. (11)–(12) into Eq. (19), applying the Fourier transform and the boundary conditions, it can be shown that

$$\bar{f}(s)=A_1(s)-A_2(s) \tag{20}$$
$$a_0[A_1(s)-A_2(s)]+B_1(s)-B_2(s)=0 \tag{21}$$
$$a_1[A_1(s)-A_2(s)]+C_1(s)-C_2(s)=0 \tag{22}$$

Substituting Eqs. (13)–(18) into Eqs. (1)–(3), it can be obtained

$$(c_{440}+a_0e_{150}+a_1q_{150})A_1(s)+e_{150}B_1(s)+q_{150}C_1(s)+(c_{440}+a_0e_{150}+a_1q_{150})A_2(s)+e_{150}B_2(s)+q_{150}C_2(s)=0 \tag{23}$$
$$\varepsilon_{110}B_1(s)+d_{110}C_1(s)+\varepsilon_{110}B_2(s)+d_{110}C_2(s)=0 \tag{24}$$
$$d_{110}B_1(s)+\mu_{110}C_1(s)+d_{110}B_2(s)+\mu_{110}C_2(s)=0 \tag{25}$$

A superposed bar indicates a Fourier transform throughout the paper. By solving the six equations (20–25) with six unknown functions and substituting the solutions into Eqs. (13)–(15) and applying the boundary conditions (1–2) to the results, one obtains

$$\frac{1}{2\pi}\int_{-\infty}^{\infty}\bar{f}(s)e^{-isx}ds=0,\quad |x|>l \tag{26}$$

$$\frac{c_{440}e^{\beta x}}{2\pi}\int_{-\infty}^{\infty}\gamma\bar{f}(s)e^{-isx}ds=\tau_0(x),\quad |x|\le l \tag{27}$$

To determine the unknown function $\bar{f}(s)$, the above pair of dual integral equations (26–27) must be solved.

4
Solution of the dual integral equations

From the natural property of the displacement along the crack line, it can be shown that the jump of the displacements across the crack surface is a finite, continuous and differentiable function. Hence, the jump of the displacements across the crack surfaces can be represented by the following series:

$$f(x)=\sum_{n=0}^{\infty}b_nP_n^{(1/2,1/2)}\left(\frac{x}{l}\right)\left(1-\frac{x^2}{l^2}\right)^{1/2},\quad \text{for } |x|\le l \tag{28}$$
$$f(x)=w^{(1)}(x,0^+)-w^{(2)}(x,0^-)=0,\quad \text{for } |x|>l \tag{29}$$

where b_n are unknown coefficients to be determined and $P_n^{(1/2,1/2)}(x)$ is a Jacobi polynomial [25]. The Fourier transform of Eqs. (28), (29) is [26]

$$\bar{f}_1(s)=\sum_{n=0}^{\infty}b_nG_n\frac{1}{s}J_{n+1}(sl),\quad G_n=2\sqrt{\pi}(-1)^ni^n\frac{\Gamma\left(n+1+\frac{1}{2}\right)}{n!} \tag{30}$$

where $\Gamma(x)$ and $J_n(x)$ are the Gamma and Bessel functions, respectively.

Substituting Eq. (30) into Eqs. (26), (27), Eq. (26) has been automatically satisfied. After integration with respect to x over the range $[-l, x]$, Eq. (27) is reduced to

$$\frac{c_{440}}{4\pi}\sum_{n=0}^{\infty} b_n G_n \int_{-\infty}^{\infty} \frac{i\gamma}{s^2} J_{n+1}(sl)[e^{-isx} - e^{isl}]ds = \int_{-l}^{x} \tau_0(s)e^{-\beta s}ds \tag{31}$$

From the relationships in Ref. [25], the semi-infinite integral in Eq. (31) can be modified to

$$\begin{aligned}\int_{-\infty}^{\infty} \frac{\gamma}{s^2} J_{n+1}(sl)[e^{-isx} - e^{isl}]ds = &\begin{cases} \frac{2}{n+1}\left\{\cos\left[(n+1)\sin^{-1}\left(\frac{x}{l}\right)\right] - (-1)^{(n+1)/2}\right\}, & n = 1, 3, 5, 7, \ldots \\ \frac{-2i}{n+1}\left\{\sin\left[(n+1)\sin^{-1}\left(\frac{x}{l}\right)\right] + (-1)^{\frac{n}{2}}\right\}, & n = 0, 2, 4, 6, \ldots \end{cases} \\ &+ \int_0^{\infty} \frac{1}{s}\left[\frac{\gamma}{s} - 1\right] J_{n+1}(sl)[e^{-isx} - e^{isl}]ds \\ &+ \int_{-\infty}^{0} \frac{1}{s}\left[\frac{\gamma}{s} + 1\right] J_{n+1}(sl)[e^{-isx} - e^{isl}]ds \end{aligned} \tag{32}$$

Thus, the semi-infinite integral in Eq. (31) can be easily evaluated numerically. Equation (31) can now be solved for the coefficients b_n by the Schmidt method [18–20]. For brevity, Eq. (31) can be rewritten as

$$\sum_{n=0}^{\infty} b_n E_n(x) = U(x), \quad -l \le x \le l \tag{33}$$

where $E_n(x)$ and $U(x)$ are known functions and the coefficients b_n are to be determined. A set of functions $P_n(x)$ that satisfy the orthogonality condition

$$\int_{-l}^{l} P_m(x)P_n(x)dx = N_n\delta_{mn}, \quad N_n = \int_{-l}^{l} P_n^2(x)dx \tag{34}$$

can be constructed from the function, $E_n(x)$, such that

$$P_n(x) = \sum_{i=0}^{n} \frac{M_{in}}{M_{nn}} E_i(x) \tag{35}$$

where M_{ij} is the cofactor of the element d_{ij} of D_n, which is defined as

$$D_n = \begin{bmatrix} d_{00}, d_{01}, d_{02}, \ldots, d_{0n} \\ d_{10}, d_{11}, d_{12}, \ldots, d_{1n} \\ d_{20}, d_{21}, d_{22}, \ldots, d_{2n} \\ \ldots\ldots\ldots\ldots \\ \ldots\ldots\ldots\ldots \\ \ldots\ldots\ldots\ldots \\ d_{n0}, d_{n1}, d_{n2}, \ldots, d_{nn} \end{bmatrix}, \quad d_{ij} = \int_{-l}^{l} E_i(x)E_j(x)dx \tag{36}$$

Using Eqs. (33)–(36), we obtain

$$b_n = \sum_{j=n}^{\infty} q_j \frac{M_{nj}}{M_{jj}} \quad \text{with } q_j = \frac{1}{N_j}\int_{-l}^{l} U(x)P_j(x)dx \tag{37}$$

5 Intensity factors

The coefficients b_n are known, so that the entire perturbation stress field, the perturbation electric displacement field and the magnetic flux can be obtained. However, in fracture mechanics, it is important to determine the perturbation stress $\tau_{yz}^{(1)}$, the perturbation electric displacement $D_y^{(1)}$ and the magnetic flux $B_y^{(1)}$ in the vicinity of the crack tips. In the case of the present study, $\tau_{yz}^{(1)}$, $D_y^{(1)}$ and $B_y^{(1)}$ along the crack line can be expressed, respectively, as

$$\tau_{yz}^{(1)}(x,0)=\tau_{yz}$$
$$=-\frac{c_{440}e^{\beta x}}{4\pi}\sum_{n=0}^{\infty}b_nG_n\int_{-\infty}^{\infty}\frac{\gamma}{s}J_{n+1}(sl)e^{-isx}ds$$
$$=-\frac{c_{440}e^{\beta x}}{4\pi}\sum_{n=0}^{\infty}b_nG_n\left[\int_{0}^{\infty}J_{n+1}(sl)e^{-isx}ds+\int_{0}^{\infty}\frac{\gamma-s}{s}J_{n+1}(sl)e^{-isx}ds\right.$$
$$\left.-\int_{-\infty}^{0}J_{n+1}(sl)e^{-isx}ds+\int_{-\infty}^{0}\frac{\gamma+s}{s}J_{n+1}(sl)e^{-isx}ds\right] \quad (38)$$

$$D_y^{(1)}(x,0)=D_y=-\frac{e_{150}e^{\beta x}}{4\pi}\sum_{n=0}^{\infty}b_nG_n\int_{-\infty}^{\infty}\frac{\gamma}{s}J_{n+1}(sl)e^{-isx}ds$$
$$=-\frac{e_{150}e^{\beta x}}{4\pi}\sum_{n=0}^{\infty}b_nG_n\left[\int_{0}^{\infty}J_{n+1}(sl)e^{-isx}ds+\int_{0}^{\infty}\frac{\gamma-s}{s}J_{n+1}(sl)e^{-isx}ds\right.$$
$$\left.-\int_{-\infty}^{0}J_{n+1}(sl)e^{-isx}ds+\int_{-\infty}^{0}\frac{\gamma+s}{s}J_{n+1}(sl)e^{-isx}ds\right] \quad (39)$$

$$B_y^{(1)}(x,0)=B_y=-\frac{q_{150}e^{\beta x}}{4\pi}\sum_{n=0}^{\infty}b_nG_n\int_{-\infty}^{\infty}\frac{\gamma}{s}J_{n+1}(sl)e^{-isx}ds$$
$$=-\frac{q_{150}e^{\beta x}}{4\pi}\sum_{n=0}^{\infty}b_nG_n\left[\int_{0}^{\infty}J_{n+1}(sl)e^{-isx}ds+\int_{0}^{\infty}\frac{\gamma-s}{s}J_{n+1}(sl)e^{-isx}ds\right.$$
$$\left.-\int_{-\infty}^{0}J_{n+1}(sl)e^{-isx}ds+\int_{-\infty}^{0}\frac{\gamma+s}{s}J_{n+1}(sl)e^{-isx}ds\right] \quad (40)$$

For $x>l$, the singular parts of the stress field, the electric displacement field and the magnetic flux can be expressed, respectively, as follows:

$$\tau_1=-\frac{c_{440}e^{\beta x}}{4\pi}\sum_{n=0}^{\infty}b_nG_n\left[\int_{0}^{\infty}J_{n+1}(sl)e^{-isx}ds-\int_{-\infty}^{0}J_{n+1}(sl)e^{-isx}ds\right]=\frac{c_{440}e^{\beta x}}{2\pi}\sum_{n=0}^{\infty}b_nG_nQ_n(x) \quad (41)$$

$$D_1=-\frac{e_{150}e^{\beta x}}{4\pi}\sum_{n=0}^{\infty}b_nG_n\left[\int_{0}^{\infty}J_{n+1}(sl)e^{-isx}ds-\int_{-\infty}^{0}J_{n+1}(sl)e^{-isx}ds\right]=\frac{e_{150}e^{\beta x}}{2\pi}\sum_{n=0}^{\infty}b_nG_nQ_n(x) \quad (42)$$

$$B_1=-\frac{q_{150}e^{\beta x}}{4\pi}\sum_{n=0}^{\infty}b_nG_n\left[\int_{0}^{\infty}J_{n+1}(sl)e^{-isx}ds-\int_{-\infty}^{0}J_{n+1}(sl)e^{-isx}ds\right]=\frac{q_{150}e^{\beta x}}{2\pi}\sum_{n=0}^{\infty}b_nG_nQ_n(x) \quad (43)$$

where

$$Q_n(x)=\begin{cases}\frac{(-1)^{n/2}l^{n+1}}{\sqrt{x^2-l^2}[x+\sqrt{x^2-l^2}]^{n+1}}, & n=0,2,4,6,\ldots\\ \frac{i(-1)^{(n+1)/2}l^{n+1}}{\sqrt{x^2-l^2}[x+\sqrt{x^2-l^2}]^{n+1}}, & n=1,3,5,7,\ldots\end{cases}$$

For $x<-l$, the singular parts of the stress field, the electric displacement field and the magnetic flux can be expressed, respectively, as follows:

$$\tau_2=-\frac{c_{440}e^{\beta x}}{4\pi}\sum_{n=0}^{\infty}b_nG_n\left[\int_{0}^{\infty}J_{n+1}(sl)e^{-isx}ds-\int_{-\infty}^{0}J_{n+1}(sl)e^{-isx}ds\right]=\frac{c_{440}e^{\beta x}}{2\pi}\sum_{n=0}^{\infty}b_nG_nQ_n^{*}(x) \quad (44)$$

$$D_2 = -\frac{e_{150}e^{\beta x}}{4\pi}\sum_{n=0}^{\infty} b_n G_n \left[\int_0^{\infty} J_{n+1}(sl)e^{-isx}ds - \int_{-\infty}^{0} J_{n+1}(sl)e^{-isx}ds\right] = \frac{e_{150}e^{\beta x}}{2\pi}\sum_{n=0}^{\infty} b_n G_n Q_n^*(x) \tag{45}$$

$$B_2 = -\frac{q_{150}e^{\beta x}}{4\pi}\sum_{n=0}^{\infty} b_n G_n \left[\int_0^{\infty} J_{n+1}(sl)e^{-isx}ds - \int_{-\infty}^{0} J_{n+1}(sl)e^{-isx}ds\right] = \frac{q_{150}e^{\beta x}}{2\pi}\sum_{n=0}^{\infty} b_n G_n Q_n^*(x) \tag{46}$$

where

$$Q_n^*(x) = \begin{cases} \frac{(-1)^{n/2} l^{n+1}}{\sqrt{x^2-l^2}[|x|+\sqrt{x^2-l^2}]^{n+1}}, & n = 0, 2, 4, 6, \ldots \\ \frac{-i(-1)^{(n+1)/2} l^{n+1}}{\sqrt{x^2-l^2}[|x|+\sqrt{x^2-l^2}]^{n+1}}, & n = 1, 3, 5, 7, \ldots \end{cases}$$

The results of the stress, the electric displacement and the magnetic flux intensity factors at the right tip of the crack, respectively, are given as follows:

$$K(l) = \lim_{x\to l^+}\sqrt{2(x-l)}\cdot\tau_1 = \frac{c_{440}e^{\beta l}}{\sqrt{\pi l}}\sum_{n=0}^{\infty}(-1)^n b_n \frac{\Gamma\left(n+1+\frac{1}{2}\right)}{n!} \tag{47}$$

$$K^D(l) = \lim_{x\to l^+}\sqrt{2(x-l)}\cdot D_1 = \frac{e_{150}e^{\beta l}}{\sqrt{\pi l}}\sum_{n=0}^{\infty}(-1)^n b_n \frac{\Gamma\left(n+1+\frac{1}{2}\right)}{n!} = \frac{e_{150}}{c_{440}}K(l) \tag{48}$$

$$K^B(l) = \lim_{x\to l^+}\sqrt{2(x-l)}\cdot B_1 = \frac{q_{150}e^{\beta l}}{\sqrt{\pi l}}\sum_{n=0}^{\infty}(-1)^n b_n \frac{\Gamma\left(n+1+\frac{1}{2}\right)}{n!} = \frac{q_{150}}{c_{440}}K(l) \tag{49}$$

The results of the stress, the electric displacement and the magnetic flux intensity factors at the left tip of the crack, respectively, are given as follows:

$$K(-l) = \lim_{x\to -l^-}\sqrt{2(|x|-l)}\cdot\tau_2 = \frac{c_{440}e^{-\beta l}}{\sqrt{\pi l}}\sum_{n=0}^{\infty} b_n \frac{\Gamma\left(n+1+\frac{1}{2}\right)}{n!} \tag{50}$$

$$K^D(-l) = \lim_{x\to -l^-}\sqrt{2(|x|-l)}\cdot D_2 = \frac{e_{150}e^{-\beta l}}{\sqrt{\pi l}}\sum_{n=0}^{\infty} b_n \frac{\Gamma\left(n+1+\frac{1}{2}\right)}{n!} = \frac{e_{150}}{c_{440}}K(-l) \tag{51}$$

$$K^B(-l) = \lim_{x\to -l^-}\sqrt{2(|x|-l)}\cdot B_2 = \frac{q_{150}e^{-\beta l}}{\sqrt{\pi l}}\sum_{n=0}^{\infty} b_n \frac{\Gamma\left(n+1+\frac{1}{2}\right)}{n!} = \frac{q_{150}}{c_{440}}K(-l) \tag{52}$$

6
Numerical calculations and discussion

As discussed in other works [18–20], it can be seen that the Schmidt method performs satisfactorily if the first ten terms of the infinite series in Eq. (33) are retained. The behavior of the sum of the series is stable with increasing number of terms in Eq. (33). In the present paper, it is assumed that the crack is only subjected to an anti-plane shear stress loading, and is not subject to an electric field or a magnetic flux loading. From Eqs. (31), (47) and (50), one deduces that the stress field does not depend on the shear modulus c_{440} but the crack length and the gradient parameter of the functionally graded piezoelectric/piezomagnetic materials. So, in all computation, the shear modulus c_{440} is not considered. The crack surface loading, $-\tau_0(x)$, will simply be assumed to be a polynomial of the form as follows:

$$-\tau_0(x) = -p_0 - p_1\left(\frac{x}{l}\right) - p_2\left(\frac{x}{l}\right)^2 - p_3\left(\frac{x}{l}\right)^3 \tag{53}$$

Since the problem is linear, the results can be superimposed in any suitable manner. The results are obtained by taking only one of the four input parameters p_0, p_1, p_2 and p_3 to be nonzero at a time. The normalized nonhomogeneity constant βl is varied between -2.8 and 2.8, which covers most practical cases. The results of the present paper are shown in Figs. 2–5. From the results, the following observations are very significant:

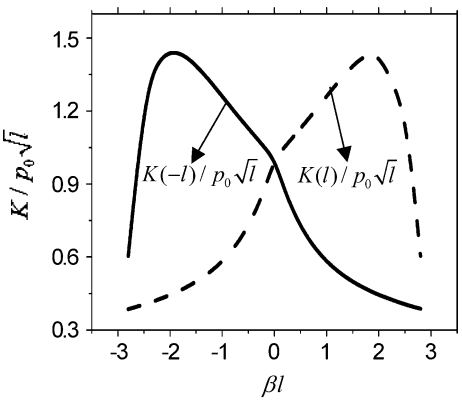

Fig. 2. Influence of βl on the stress intensity factors under the loading $\tau_0(x) = p_0$

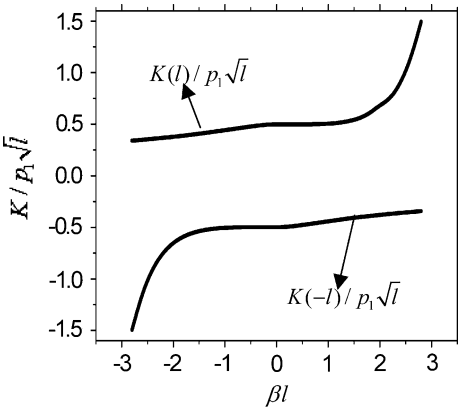

Fig. 3. Influence of βl on the stress intensity factors under the loading $\tau_0(x) = p_1 x$

(i) From the results, it can be shown that the singular stress, the singular electric displacement and the singular magnetic flux in functionally graded piezoelectric/piezomagnetic materials have the same forms as those in homogeneous piezoelectric/piezomagnetic materials or in homogeneous piezoelectric materials for the anti-plane shear fracture problem, but the magnitudes of the intensity factors depend significantly upon the gradient parameter of the functionally graded piezoelectric/piezomagnetic materials, as discussed in [17].

(ii) From Eqs. (31), (47) and (50), it can be obtained that the stress field does not depend on the shear modulus c_{440} but the crack length and the gradient parameters of the functionally graded piezoelectric/piezomagnetic materials. The stress intensity factor depends on the nonhomogeneity parameter βl. This is the same as the anti-plane shear fracture problem in general nonhomogeneous elastic materials. However, the electric displacement and the magnetic flux intensity factors depend on the nonhomogeneity parameter βl and the properties of the magneto-electro-elastic composite materials. The electro-magneto-elastic coupling effects can be obtained, as shown in Eqs. (47)–(52).

(iii) The solution of this problem can be reduced to that of homogeneous piezoelectric/piezomagnetic materials for $\beta l = 0$. From the results, it can be shown that the stress intensity factor is equal to unity when $\beta l = 0$ for a loading of $\tau_0(x) = p_0$, as shown in Figure 2. It can also be shown that the stress intensity factor is equal to 0.5 when $\beta l = 0$ for a loading of $\tau_0(x) = p_1(x/l)$, as shown in Fig. 3. This is consistent with the fracture problem in general elastic materials for the anti-plane shear fracture problem. It has also been proved that the Schmidt method can be used to solve this problem.

(iv) For the symmetric loading, the stress intensity factors at crack tips are symmetric about the line $\beta l = 0$, as shown in Figs. 2 and 4. However, for the antisymmetric loading, the stress intensity factors at crack tips are symmetric about the point $K = 0$ and $\beta l = 0$, as shown in Figs. 3 and 5.

(v) For the symmetric loading, as shown in Figs. 2 and 4, the stress intensity factor at the right tip of the crack tends to increase with an increase in the functionally graded parameter βl, until reaching a maximum at $\beta l = 1.5$, and then decreases in magnitude. However, the stress intensity factor at the left tip of the crack tends to increase with an increase in the functionally graded parameter βl, until reaching a maximum at $\beta l = -1.5$, and then decreases in magnitude.

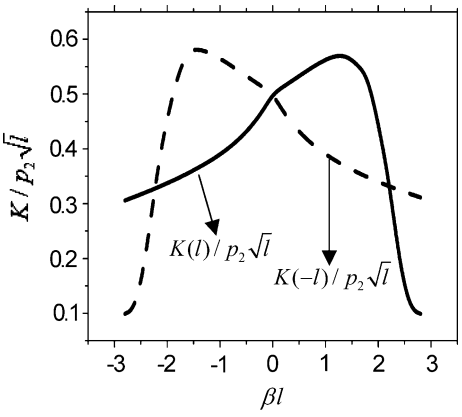

Fig. 4. Influence of βl on the stress intensity factors under the loading $\tau_0(x) = p_2 x^2$

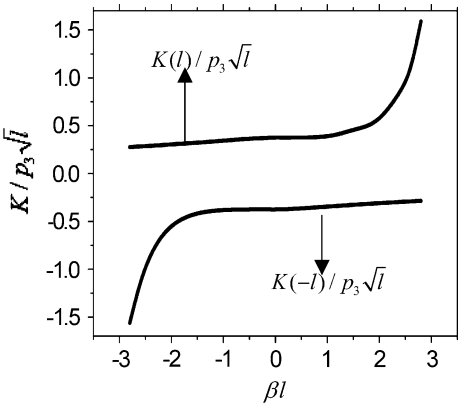

Fig. 5. Influence of βl on the stress intensity factors under the loading $\tau_0(x) = p_3 x^2$

(vi) For the antisymmetric loading, as shown in Figs. 3 and 5, the stress intensity factor at the right tip of the crack tends to increase slowly with an increase in the functionally graded parameter βl until $\beta l = 2.0$, and then increases rapidly in magnitude. However, the stress intensity factor at the left tip of the crack tends to increase rapidly with an increase in the functionally graded parameter βl until $\beta l = -2.0$, and then increases slowly in magnitude. Hence, stress intensity factors can be reduced by adjusting the functionally graded parameter βl according to the form of the loading. These phenomena are caused by the changing of the functionally graded parameter βl. The curves of the stress intensity factor $K(l)$ in Figs. 3 and 5 are similar to the exponential curve.

(vii) The results of the electric displacement and the magnetic flux intensity factors can be directly obtained form the results of the stress intensity factors through Eqs. (47)–(52). For the electric displacement and the magnetic flux intensity factors, they follow the same rules as the stress intensity factor shown in Eqs.(47)–(52). In the present paper, they are omitted.

References

1. **Wu, T.L.; Huang, J.H.:** Closed-form solutions for the magnetoelectric coupling coefficients in fibrous composites with piezoelectric and piezomagnetic phases. Int J Solids Struct 37 (2000) 2981–3009
2. **Sih, G.C.; Song, Z.F.:** Magnetic and electric poling effects associated with crack growth in $BaTiO_3$-$CoFe_2O_4$ composite. Theor Appl Fracture Mech 39 (2003) 209–227
3. **Song, Z.F.; Sih, G.C.:** Crack initiation behavior in magnetoelectroelastic composite under in-plane deformation. Theor Appl Fracture Mech 39 (2003) 189–207
4. **Van Suchtelen, J.:** Product properties: a new application of composite materials. Phillips Res Rep 27 (1972) 28–37
5. **Harshe, G.; Dougherty, J.P.; Newnham, R.E.:** Theoretical modeling of 3–0/0–3 magnetoelectric composites. Int J Appl Electromagnetics Mater 4 (1993) 161–171
6. **Avellaneda, M.; Harshe, G.:** Magnetoelectric effect in piezoelectric/magnetostrictive multiplayer (2–2) composites. J Intell Mater Syst Struct 5 (1994) 501–513
7. **Nan, C.W.:** Magnetoelectric effect in composites of piezoelectric and piezomagnetic phases. Phys Rev B 50 (1994) 6082–6088
8. **Benveniste, Y.:** Magnetoelectric effect in fibrous composites with piezoelectric and magnetostrictive phases. Phys Rev B 51 (1995) 16424–16427

9. **Huang, J.H.; Kuo, W.S.:** The analysis of piezoelectric/piezomagnetic composite materials containing ellipsoidal inclusions. J Appl Phys 81(3) (1997) 1378–1386
10. **Li, J.Y.:** Magnetoelectroelastic multi-inclusion and inhomogeneity problems and their applications in composite materials. Int J Eng Sci 38 (2000) 1993–2011
11. **Takagi, K.; Li, J.F.; Yokoyama, S.; Watanabe, R.:** Fabrication and evaluation of PZT/Pt piezoelectric composites and functionally graded actuators. J Eur Ceramic Soc 10 (2003) 1577–1583
12. **Jin, D.R.:** Functionally graded PZT/ZnO piezoelectric composites. J Mater Sci Lett 22 (2003) 971–974
13. **Chen, J.; Liu, Z.X.; Zou, Z.Z.:** Electriomechanical impact of a crack in a functionally graded piezoelectric medium. Theor Appl Fracture Mech 39 (2003) 47–60
14. **Jin, B.; Zhong, Z.:** A moving mode-III crack in functionally graded piezoelectric material: permeable problem. Mech Res Commun 29 (2002) 217–224
15. **Wang, B.L.:** A mode-III crack in functionally graded piezoelectric materials. Mech Res Commun 30 (2003) 151–159
16. **Soon Man Kwon.:** Electrical nonlinear anti-plane shear crack in a functionally graded piezoelectric strip. Int J Solids Struct 40 (2003) 5649–5667
17. **Weng, G.J.; Li, C.Y.:** Anti-plane crack problem in functionally graded piezoelectric materials. J Appl Mech 69(4) (2002) 481–488
18. **Morse, P.M.; Feshbach, H.:** Methods of theoretical physics, Vol. 1. McGraw-Hill, New York, 1958
19. **Zhou, Z.G.; Han, J.C.; Du, S.Y.:** Investigation of a Griffith crack subject to anti-plane shear by using the non-local theory. Int J Solids Struct 36 (1999) 3891–3901
20. **Zhou, Z.G., Wang, B.:** The behavior of two parallel symmetry permeable interface cracks in a piezoelectric layer bonded to two half piezoelectric materials planes. Int J Solids Struct 39(17) (2002) 4485–4500
21. **Soh, A.K.; Fang, D.N.; Lee, K.L.:** Analysis of a bi-piezoelectric ceramic layer with an interfacial crack subjected to anti-plane shear and in-plane electric loading. Eur J Mech A/Solid 19 (2000) 961–977
22. **Delale, F.; Erdogan, F.:** On the mechanical modeling of the interfacial region in bonded half-planes. ASME J Appl Mech 55 (1988) 317–324
23. **Fildis, H.; Yahsi, O.S.:** The axisymmetric crack problem in a non-homogeneous interfacial region between homogeneous half-spaces. Int J Fracture 78 (1996) 139–163
24. **Ozturk, M.; Erdogan, F.:** (1997), Mode I crack problem in an inhomogeneous orthotropic medium, Int J Eng Sci 35 (1997) 869–883
25. **Gradshteyn, I.S.; Ryzhik, I.M.:** Table of integral, series and products. Academic New York, 1980
26. **Erdelyi, A.:** (ed) Tables of integral transforms, Vol. 1, McGraw–Hill, New York, 1954